The Astrophysical Journal, 651:853–860, 2006 November 10


# CO DETECTION AND MILLIMETER CONTINUUM EMISSION FROM LOW SURFACE BRIGHTNESS GALAXIES

Mousumi Das,[1,2] Karen O'Neil,[3] Stuart N. Vogel,[2] and Stacy McGaugh[2]
*Received 2006 March 3; accepted 2006 June 26*

## ABSTRACT

We present BIMA and IRAM CO (1–0) observations of seven low surface brightness (LSB) galaxies, including three large spiral galaxies with faint disks but prominent bulges and four relatively small LSB galaxies with irregular disks. The giant LSB galaxies are UGC 5709, UGC 6614, and F568-6 (Malin 2). The smaller LSB galaxies are NGC 5585, UGC 4115, UGC 5209, and F583-1. The galaxies were selected based on their relatively high metallicity and apparent signs of star formation in their disks. The BIMA maps suggested the presence of molecular gas in two of the giant LSB galaxies: F568-6 and UGC 6614. Using the 30 m IRAM telescope, we detected CO (1–0) emission in the disks of both galaxies and in the nucleus of F568-6. The molecular gas in these galaxies is clearly offset from the nucleus and definitely associated with the LSB disk. In addition, we detected a millimeter continuum source in the center of UGC 6614. When compared with Very Large Array (VLA) 1.5 GHz observations of the galaxy, the emission was found to have a flat spectrum, indicating that the millimeter continuum emission is most likely due to an active galactic nucleus (AGN) in the galaxy. Our results show that giant LSB spiral galaxies may contain significant quantities of molecular gas in their disks and also harbor radio-bright AGNs in their centers.

*Subject headings:* galaxies: individual (F568-6, UGC 6614) — galaxies: ISM — ISM: kinematics and dynamics — ISM: molecules — radio lines: galaxies

## 1. INTRODUCTION

Low surface brightness (LSB) galaxies have faint stellar disks of central brightness less than 23 $B$ mag arcsec$^{-2}$ (Impey & Bothun 1997). Although they have diffuse stellar disks, they are extremely gas-rich, with large H I gas disks that extend well beyond their apparent stellar disks. The high gas fraction observed in these galaxies, combined with the overall low metallicity, suggests that they have had much less star formation compared to regular high surface brightness (HSB) galaxies, probably because their gas surface densities are well below the critical value required for star formation (van der Hulst et al. 1993). They are thus considered to be less evolved compared to HSB galaxies. They also have very large mass-to-light ratios, which indicates that their disks are dominated by massive dark matter halos; the massive halo inhibits the formation of disk instabilities, such as bars and spiral perturbations, which further contributes to the overall low star formation rate in these galaxies.

LSB galaxies span a wide range of Hubble type and size but can be roughly divided into two categories. The first category is made up of the very populous dwarf spiral and dwarf irregular galaxies. The majority of LSB galaxies in our local universe are of this type. The second category comprises late-type spiral galaxies that are very large in size; some may have prominent bulges and discernible spiral arms. These so-called LSB giants, such as Malin 1 and UGC 6614, are relatively rare. The origin and evolution of these faint galaxies is still not clear. Previous studies suggest that LSB galaxies are relatively isolated compared to other types of galaxies, and the lack of galaxy interaction has left them less evolved compared to their HSB counterparts. To obtain a better understanding of their evolution, we need to understand their star formation history. An important step in this direction is to determine the gas distribution in their disks.

Although LSB galaxies are rich in H I, molecular gas ($H_2$) has been detected in only a handful of such galaxies (O'Neil et al. 2000, 2003; Matthews & Gao 2001; O'Neil & Schinnerer 2004; Matthews et al. 2005). The low detection rate is probably a combination of several factors, such as a low dust content, low metallicity, and a low surface density of neutral gas (de Blok & van der Hulst 1998), all of which impede gas cooling, molecule formation, and cloud condensation. However, modest amounts of ongoing star formation have been observed in most late-type galaxies (McGaugh & Bothun 1994; McGaugh et al. 1995; Matthews & Gallagher 1997), which must mean that star formation can proceed even in these adverse environments. Very little is known about the physics of star formation in such low-density and low-metallicity environments. One possibility is that star formation occurs in localized regions over the disk. Molecular gas is then patchy in distribution and hence difficult to detect.

To address some of these issues, we searched for molecular gas in seven LSB galaxies. Three of the galaxies are LSB giants, and the remaining four are smaller late-type galaxies. The parameters of the galaxies are listed in Table 1. All the galaxies in our sample have relatively high metallicities and show signs of star formation in their disks. We followed up tentative Berkeley-Illinois-Maryland Association (BIMA) detections of CO (1–0) emission with IRAM 30 m single-dish observations. CO (1–0) emission was detected in two galaxies: F568-6 (Malin 2) and UGC 6614. The molecular gas masses were derived from the IRAM fluxes; they represent gas masses for the detected regions only and not for the entire galaxy. We also detected millimeter continuum emission from the nucleus of one galaxy in our sample: UGC 6614. The emission was detected at a mean frequency of 111.2 GHz and is most likely due to an AGN in the galaxy.

In the following sections we present our observations and discuss the implications of our results. For F568-6 (Malin 2), which has a fairly high redshift ($z = 0.046$), we adopt a luminosity distance of $D_L = 198.8$ Mpc ($H_0 = 71$ km s$^{-1}$ Mpc$^{-1}$); this leads to a scale of 0.92 kpc arcsec$^{-1}$. UGC 6614 has a much lower redshift, and so we adopt the angular distance of $D = 89.5$ Mpc

[1] Raman Research Institute, Sadashivanagar, Bangalore 560 080, India; mousumi@rri.res.in.
[2] Department of Astronomy, University of Maryland, College Park, MD 20742.
[3] NRAO, P.O. Box 2, Green Bank, WV 24944.

TABLE 1
Galaxy Sample

| Galaxy Name | Galaxy Type | Velocity (km s$^{-1}$) | R.A. (J2000.0) | Decl. (J2000.0) | $D_{25}$[a] (arcsec) | Inclination[b] (deg) |
|---|---|---|---|---|---|---|
| UGC 5709 | Sd | 6206 | 10 31 16.2 | +19 22 59 | 80.9 | 54.6 |
| UGC 6614 | (R)SA(r)a | 6351 | 11 39 14.8 | +17 08 37 | 99.6 | 29.9 |
| F568-6 | Sd/p | 13820 | 10 39 52.5 | +20 50 49 | ... | 38.0 |
| NGC 5585 | SAB(s)d | 305 | 14 19 48.2 | +56 43 45 | 345.3 | 53.2 |
| UGC 4115 | IAm | 338 | 07 57 01.8 | +14 23 27 | 109.2 | 67.1 |
| UGC 5209 | Im | 538 | 09 45 04.2 | +32 14 18 | 54.7 | 0.0 |
| F583-1 | Sm/Irr | 2264 | 15 57 27.5 | +20 39 58 | 42.0 | 63.0 |

Note.—Units of right ascension are hours, minutes, and seconds, and units of declination are degrees, arcminutes, and arcseconds.
[a] The $D_{25}$ diameters for all the galaxies are from the RC3 catalog, except for F583-1, which is from de Blok et al. (1996).
[b] The inclinations for all the galaxies except F568-6 and F583-1 are from the HyperLeda catalog (Paturel et al. 2003). For F568-6, the inclination is from Pickering et al. (1997), and for F583-1 the inclination is obtained from de Blok et al. (1996).

($V_{sys} = 6351$ km s$^{-1}$), which leads to a distance scale of 0.43 kpc arcsec$^{-1}$.

## 2. OBSERVATIONS

### 2.1. *Galaxy Sample*

Our sample of seven galaxies is listed in Table 1. To cover the range of galaxy types, we included in our sample both the large LSB spiral galaxies and the smaller LSB galaxies that have irregular disks. In addition, to improve the chances of molecular gas detection, we chose galaxies that had either relatively high metallicities or showed signs of star formation. Three of the galaxies in the sample —UGC 5709, UGC 6614, and F568-6—are giant LSB galaxies. They are large, late-type spiral galaxies with diffuse stellar disks but extended H I gas disks. Of these three galaxies, UGC 6614 and F568-6 represent the prototypical giant LSB galaxies (Quillen & Pickering 1997). Both are relatively bright and nearly face-on, and have prominent bulges and relatively strong spiral arms (McGaugh et al. 1995). The H I gas distribution and kinematics for both galaxies have been observed by Pickering et al. (1997). UGC 6614 has a ringlike feature around the bulge (Fig. 1) that is prominent even in H$\alpha$ (McGaugh et al. 1995). It has perhaps the highest metallicity known for an LSB galaxy and is estimated as log (O/H) = $-3$ to $-2.84$, which is close to solar in value (McGaugh 1994). Its nucleus shows AGN activity at optical wavelengths (Schombert 1998) and appears as a bright core in X-ray emission (*XMM-Newton* archival data). F568-6, like UGC 6614, has a massive bulge and spiral structure; in addition, it has several bright H II regions distributed over its inner disk. It also has a relatively high metallicity of log (O/H) = $-3.22$, which is basically solar in value (de Blok & van der Hulst 1998). The H I velocity field has high velocities at one position near the center, which is associated with star formation and may be due to the accretion of a dwarf (Pickering et al. 1997). This galaxy also shows signs of AGN activity at optical wavelengths (Schombert 1998), and its core has been detected in X-ray emission (*XMM-Newton* archival data). UGC 5709 has a less regular structure than the former two galaxies and is intermediate in surface brightness. Its metallicity is log (O/H) = $-3$ to $-3.2$, which is approximately solar (de Blok & van der Hulst 1998). Like F568-6 it has H II regions in the disk that have relatively high metallicities (McGaugh et al. 1995).

The other four galaxies are either dwarf or irregular galaxies that also have relatively high metallicities or signs of star formation in their disks. They are NGC 5585, UGC 4115, UGC 5209, and F583-1. Apart from F583-1, all the other galaxies are members of groups of galaxies. NGC 5585 is a companion to the bright barred galaxy M101 and has H II regions distributed over the disk. Both UGC 4115 and UGC 5209 are members of loose groups of dwarf galaxies and have irregular morphologies. F583-1 is the only distant galaxy in our sample of dwarf galaxies. It has a metallicity of log (O/H) $\sim -4$ that is substantially subsolar (de Blok & van der Hulst 1998). It also has a fairly symmetric H I morphology (de Blok et al. 1996).

### 2.2. *BIMA Observations*

We observed the sample of galaxies with the BIMA interferometer (Welch et al. 1996) in the D array from 2002 September to 2003 August. The observations were all done in single-pointing mode with a 100″ field of view centered on the galaxy nucleus. The galaxies were observed in the CO (1–0) emission line, with the line positioned in the upper sideband for all seven galaxies. UGC 5709, UGC 6614, and F568-6 have fairly significant redshifts; the remaining four galaxies have low redshifts. We used nearby radio sources for phase calibration; these are listed in Table 2. For flux calibration we used a nearby planet (e.g., Mars) or a radio source whose flux is frequently monitored (3C 273).

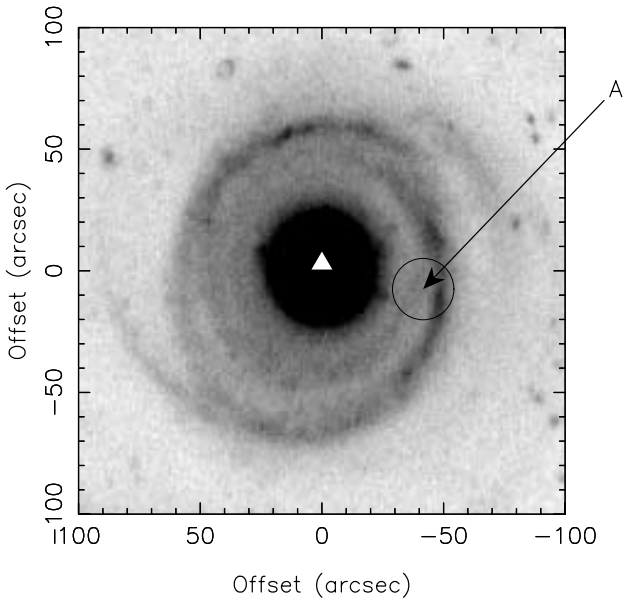


Fig. 1.—The *R*-band optical image of UGC 6614; the location of the center of the IRAM beam is indicated with the arrow labeled A. The telescope pointing center is well away from the center of the galaxy. The IRAM beam size is 22″, and the 2MASS center of the galaxy is marked with a triangle.

TABLE 2
BIMA Observations

| Galaxy Name | CO (1–0) Frequency (GHz) | Phase Calibrator | Flux Calibrator | Beam Size (arcsec) | Number of Tracks |
|---|---|---|---|---|---|
| UGC 5709 | 112.93 | 1058+015 | 3C 273 | 18.5 × 14.5 | 3 |
| UGC 6614 | 112.88 | 1118+125 | Mars | 17.3 × 15.0 | 3 |
| F568-6 | 110.19 | 1058+015 | 3C 273 | 18.4 × 16.5 | 6 |
| NGC 5585 | 115.15 | 1419+543 | Mars | 17.3 × 13.9 | 3 |
| UGC 4115 | 115.14 | 0750+125 | Mars | 17.3 × 14.6 | 1 |
| UGC 5209 | 115.07 | 0927+390 | W3OH | 16.9 × 13.8 | 2 |
| F583-1 | 114.41 | 1540+147 | Mars | 16.4 × 15.7 | 1 |

The data were reduced using the MIRIAD software package (Sault et al. 1995). We used CLEAN and natural weighting for all our maps. The typical beam size for our maps was 15″ (see Table 2 for details).

We searched through the channel maps of each galaxy in our sample for signs of CO (1–0) line emission (with velocity resolution of ~6 km s$^{-1}$). We also constructed the velocity-integrated CO (1–0) emission map by taking the zeroth moment of the CO (1–0) emission. Our data suggest that two galaxies, UGC 6614 and F568-6, have CO (1–0) emission originating from their disks. However, the emission lines for both galaxies were narrow and noisy. Thus, these observations were only an indication that molecular gas may be present in these galaxies. We did not see any CO (1–0) emission in the remaining five galaxies. However, our nondetections put upper limits for the CO (1–0) flux one could expect from these galaxies.

In addition to searching for CO (1–0) line emission in the BIMA data, we looked for millimeter continuum emission from all seven galaxies in the sample. To do this we flagged channels that might contain CO (1–0) line emission; the data flagging is based on the velocity distribution of H I emission. We then recomputed the continuum channels from the narrowband data set. Then we averaged the upper and lower sideband data to obtain the combined data set. We again used CLEAN and natural weighting to derive the continuum emission maps.

### 2.3. *IRAM* CO *Observations*

To confirm the possible detections by BIMA of molecular gas ($H_2$) in these two galaxies, we observed them with the IRAM 30 m single-dish telescope at positions close to the BIMA tentative detections. UGC 6614 and F568-6 were observed in the CO (1–0) and (2–1) emission lines using the IRAM 30 m telescope in 2004 October–November of as part of the IRAM 30 m pool observations. Table 3 lists the adopted positions, frequencies, and total time each position was observed. The beams were centered at the positions given in the table and are 22″ at 110 GHz and 11″ at 220 GHz. The positions for IRAM pointing were chosen based on the tentative BIMA CO (1–0) line detections described in § 2.2. Pointing and focus were checked every 2–3 hr, depending on the weather conditions, and pointing was found to be within the telescope limits (better than 2″). For each source both transitions were observed simultaneously with both frequencies and two (circular) polarizations. The back end was set using the 1 MHz filter bank for each polarization for the 1 mm lines and the 4 MHz filter bank for each of the 3 mm lines. The observed resolution of the 1 and 3 mm lines were 3.3 and 5.3 km s$^{-1}$, respectively.

For data reduction, the lines were smoothed over seven channels to 23 km s$^{-1}$ and over five channels to 27 km s$^{-1}$ resolution, for the CO $J = 1–0$ and 2–1 lines, respectively, using the boxcar smoothing algorithm. The maximal beam throw of 240″ was used for these observations. The image sideband rejection ratios were measured to be >30 dB for the 3 mm SIS receivers and >12 dB for the 1.3 mm SIS receivers. The data were calibrated using the standard chopper wheel technique and are reported in main-beam brightness temperature $T_{MB}$. Typical system temperatures during the observations were 160–180 and 170–250 K in the 3 and 1.3 mm bands, respectively. All data reduction was done using the Continuum and Line Analysis Single-dish Software (CLASS) developed by the Observatoire de Grenoble and IRAM (Buisson 2002).

## 3. RESULTS

### 3.1. CO (1–0) *Emission from UGC 6614 and F568-6*

Our BIMA observations suggested the presence of molecular gas at one location in the disk of UGC 6614 (Figs. 1 and 2) and at two positions in the disk of F568-6 (Figs. 3, 4, and 5). As described above, we followed up these observations with IRAM single-dish observations centered near the BIMA tentative detections. We detected CO (1–0) emission from the inner disk of both UGC 6614 and F568-6. We did not detect any emission from the remaining five galaxies; however, the BIMA maps yield upper limits to the expected molecular gas masses in these galaxies. In the following paragraphs we discuss the results for each galaxy in more detail.

*UGC 6614.*—BIMA observations of UGC 6614 indicated that there may be CO (1–0) line emission originating from the disk of UGC 6614 at approximately 38″ west of the nucleus (Fig. 1). The

TABLE 3
IRAM Observations

| Galaxy Name | R.A. (J2000.0) | Decl. (J2000.0) | CO (1–0) Frequency (GHz) | CO (2–1) Frequency (GHz) | Time (minutes) |
|---|---|---|---|---|---|
| F568-6a | 10 39 55 | 20 50 54 | 110.20559 | 220.40696 | 134 |
| F568-6b | 10 39 53 | 20 50 50 | 110.31817 | 220.63212 | 240 |
| UGC 6614 | 11 39 12 | 17 08 31 | 112.89500 | 225.78569 | 184 |

Note.—Units of right ascension are hours, minutes, and seconds, and units of declination are degrees, arcminutes, and arcseconds.

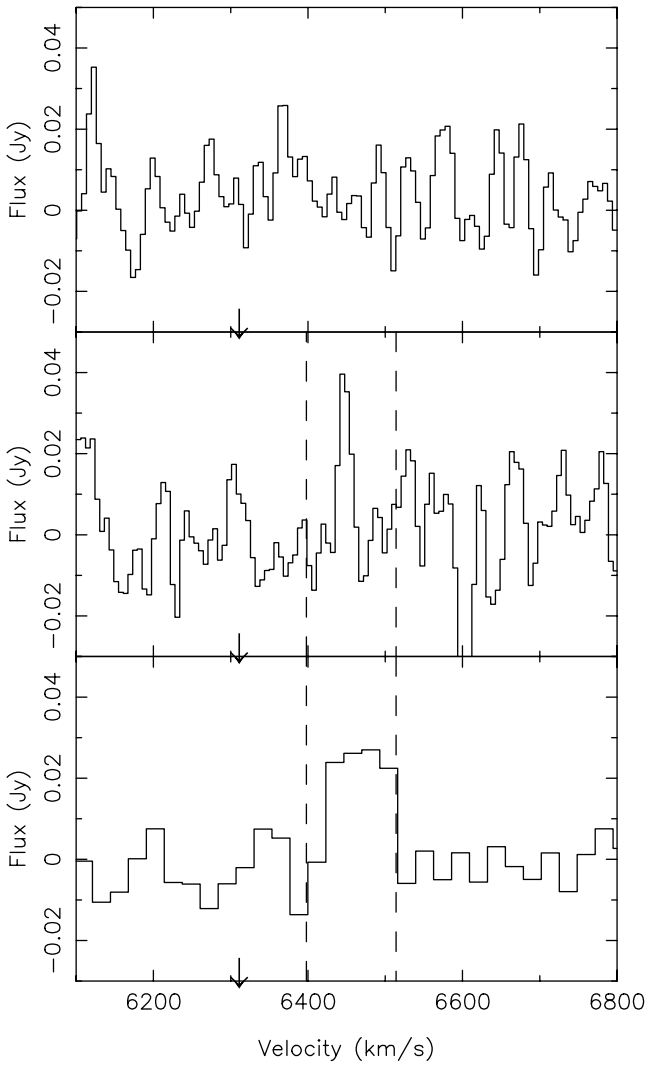


FIG. 2.—BIMA and IRAM CO (1–0) emission lines observed in UGC 6614. The top panel is a CO spectrum observed by BIMA from the nuclear region; no CO (1–0) emission is seen here. The middle panel shows the BIMA CO (1–0) spectrum observed from location A, which lies west of the nucleus and in the LSB disk. Both spectra have been smoothed to a velocity resolution of 6 km s$^{-1}$. The bottom panel is the IRAM single-dish CO (1–0) spectrum smoothed to a velocity resolution of 27 km s$^{-1}$. The systemic velocity of the galaxy is marked on the *x*-axis with an arrow. The dashed lines show the approximate width of the single-dish emission line.

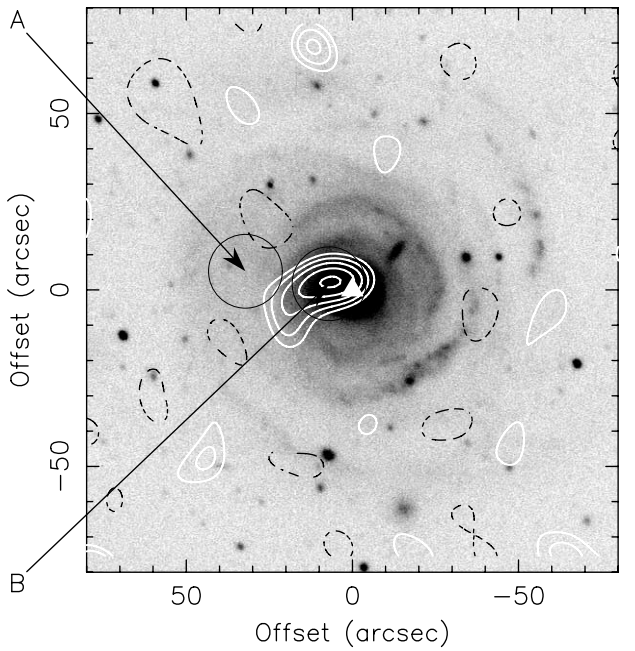


FIG. 3.—Contours of BIMA CO (1–0) line emission overlaid on the *R*-band optical image of F568-6 (Malin 2). The intensity contours in white are at 1.5, 2, 2.5, 3, and 3.5 times the rms noise level, and the contours in black are at −1.5 and −2.0 times the rms noise level. The beam is ∼17″. The pointing centers of the 22″ IRAM beams for the two CO (1–0) emission detections are indicated with the arrows labeled A and B. The 2MASS center of the galaxy is marked with a triangle.

emission is weak, and so the intensity map does not reveal much about the molecular gas distribution; hence, we did not overlay it on the optical image of the galaxy shown in Figure 1. However, although the line is weak (S/N ∼ 3.6) (Fig. 2*a*), the velocity of the line is similar to the H I line velocity at that point. In the H I map of Pickering et al. (1997) the H I velocity is between 6400 and 6420 km s$^{-1}$; this matches well with the BIMA line. Figure 1 also shows the IRAM pointing center, which is offset from the galaxy center by 38″, and the IRAM beam, which has a FWHM size of 22″. The IRAM observations detected a significant amount of CO (1–0) flux (Fig. 2*b*); no emission in the CO (2–1) line was detected. The emission is clearly offset from the galaxy center. Thus, the BIMA observations suggest that there may be significant CO (1–0) emission from the LSB disk, west of the nucleus and near the spiral arm/ring about the bulge. There may be molecular gas in the nucleus, but it is too weak to be detected with BIMA. The molecular gas in the disk appears to be associated with a spiral arm and extended along it. The IRAM observations confirm the presence of gas in the disk. The CO emission may be associated with star formation knots in the inner ring. To derive the molecular gas mass from the single-dish CO flux, we used the standard conversion factor, which gives the molecular mass as $M_{\rm mol} = 1.5 \times 10^4 D^2_{\rm Mpc} S_{\rm CO}\ M_\odot$, where $D_{\rm Mpc}$ is the galaxy distance in megaparsecs and $S_{\rm CO}$ is the velocity integrated flux in Jy km s$^{-1}$ (Strong et al. 1988; Scoville & Sanders 1987). The total molecular gas mass observed in the disk from this region is $\sim 2.8 \times 10^8\ M_\odot$ (Table 4).

*F568-6*.—BIMA observations of F568-6 suggested that there may be CO (1–0) emission originating from two positions in the inner disk of the galaxy. One position was close to the nucleus (F568-6B), and the other was clearly offset from the nucleus and close to a spiral feature in the disk (F568-6A). Although the emission lines seen in the BIMA data were relatively weak, the velocities of the lines match observed H I velocities at both positions and hence appear to be real. Figure 3 shows the BIMA CO intensity map superimposed on the *R*-band image of the galaxy. The IRAM pointings were at two locations in the disk and are marked as A and B in the figure; they are offset by ∼35″ and ∼7″, respectively, from the galaxy center. Also shown is the IRAM beam, which has a FWHM of 22″.

The IRAM CO (1–0) emission from position A (Fig. 4) has a line velocity of approximately 13,990 km s$^{-1}$. This matches the H I velocity observed at that position by Pickering et al. (1997), which lies between 13,980 and 14,020 km s$^{-1}$. The corresponding BIMA line (Fig. 4*a*) is at a velocity of ∼14,010 km s$^{-1}$, which is slightly offset from the center of the IRAM line (Fig. 4*b*). This may be because the molecular gas is distributed as clumps over the beam rather than a large gas cloud. Our BIMA observations are thus picking up emission from one bright spot, whereas the IRAM beam is sensitive to emission from the entire cloud complex. The emission from A is clearly positioned away from the galaxy nucleus; it lies to the east of the galaxy center and

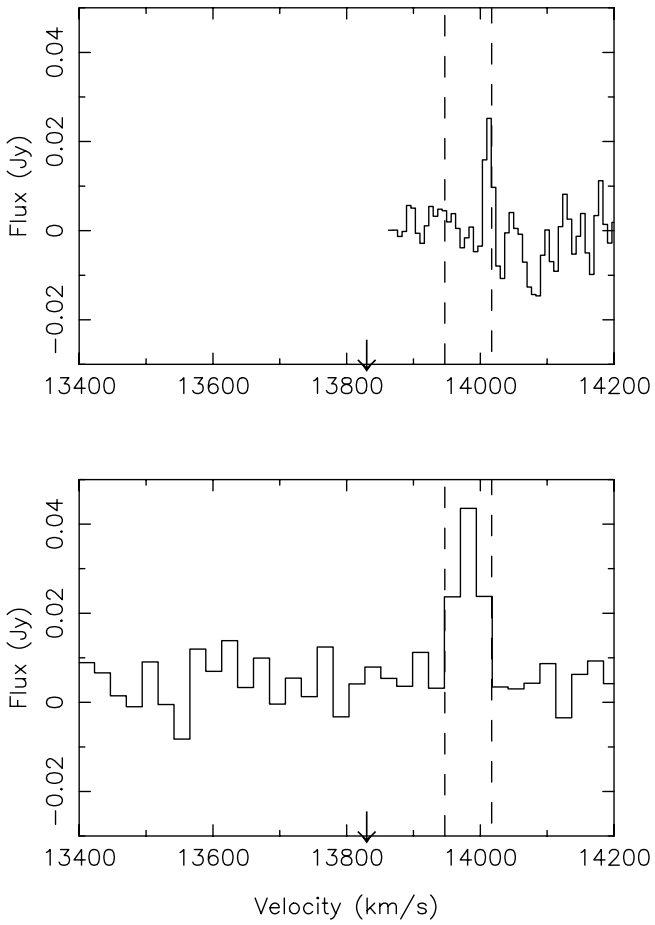


FIG. 4.—BIMA and IRAM CO (1–0) emission lines observed in F568-6 from the location marked A in Fig. 3 (i.e., approximately 35″ west of the nucleus). The top panel shows the BIMA CO (1–0) spectrum smoothed to a velocity resolution of 6 km s$^{-1}$; the bottom panel shows the IRAM single-dish CO (1–0) spectrum smoothed to a velocity resolution of 27 km s$^{-1}$. The systemic velocity of the galaxy is marked on the $x$-axis with an arrow. The dashed lines show the approximate width of the single-dish emission line.

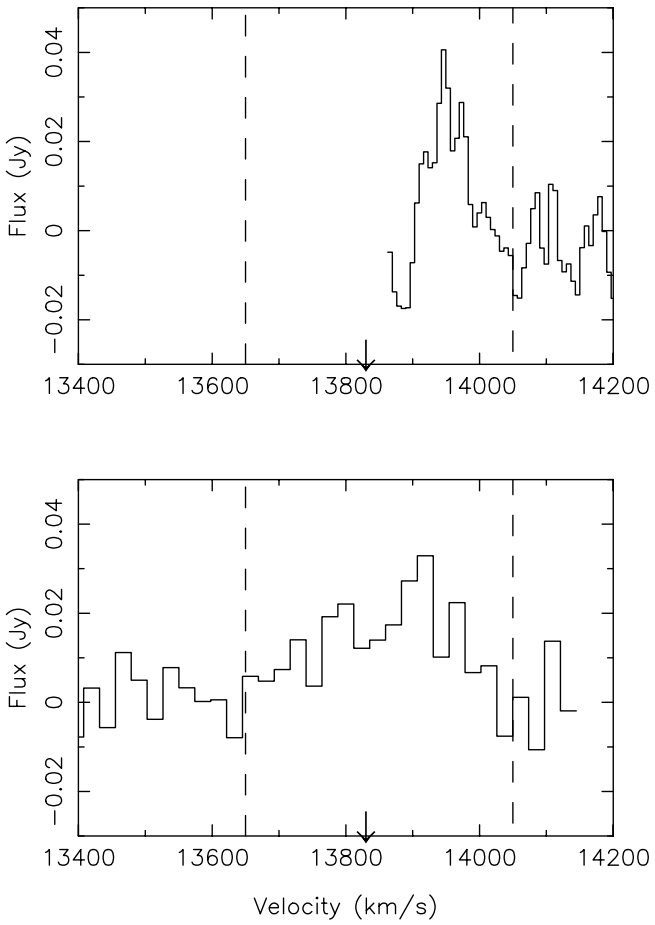


FIG. 5.—Same as Fig. 4, but for the BIMA and IRAM CO (1–0) emission lines observed in F568-6 from the location marked B in Fig. 3 (i.e., close to the nucleus).

appears to be associated with a tightly wound spiral arm emerging from the edge of the bulge. The IRAM CO (1–0) emission from position B has a peak velocity of approximately 13,910 km s$^{-1}$ (Fig. 5), and the H I velocity at that position is between 13,900 and 13,920 km s$^{-1}$ (Pickering et al. 1997). This emission appears to be associated with the nucleus. For this position, the BIMA and IRAM line velocities are fairly well matched (Figs. 5*a* and 5*b*).

To derive the molecular gas masses we used the CO luminosity $L'_{\rm CO}$, i.e., $M_{\rm mol} = \alpha L'_{\rm CO}\ M_\odot$, where $\alpha = 4\ M_\odot\ ({\rm K\ km\ s^{-1}\ pc^2})^{-1}$ (Strong et al. 1988; Scoville & Sanders 1987). The total molecular gas mass derived from summing up the gas detected at both positions A and B using the IRAM CO (1–0) flux is $\sim 2.6 \times 10^9\ M_\odot$ (Table 4). The emission is extended east of the galaxy center, but the molecular gas may well be extended west of the nucleus as well (Fig. 3). This is because the correlator setup for this galaxy did not cover the full range of velocities for which H I emission has been detected in this galaxy, since the lower edge of the correlator band was set at 13,860 km s$^{-1}$. Thus, our present detection is only a lower limit to the molecular gas distribution in F568-6 and is based only on the redshifted half of the galaxy. Hence, the molecular gas may be much more extended in the inner disk of the galaxy than our present observations indicate. In the near future we plan to map the extended molecular gas distribution in this galaxy in much better detail.

*Remaining galaxies*.—We did not detect any CO (1–0) emission from the remaining five galaxies in our sample (i.e., UGC 5709, NGC 5585, UGC 4115, UGC 5209, and F583-1). Of these, one is a giant LSB galaxy (UGC 5709), and the others are dwarf galaxies. However, we have used the noise levels in the BIMA maps to derive upper estimates of the molecular gas masses in these galaxies (Table 4) using the approximation $S_{\rm CO} = ({\rm noise})(\delta v)(N_b)$, where $\delta v$ represents the maximum width of the expected CO (1–0) emission line; $N_b$ is number of beams in the 44″ BIMA primary beam (i.e., 44 arcsec$^2$/$b_1 b_2$), and $b_1, b_2$ are the beam sizes. For $\delta v$ we have used the width of the H I line ($W_{50}$) as an upper estimate. Upper limits to the molecular gas masses are calculated from the flux using the previously mentioned formula $M_{\rm mol} = 1.5 \times 10^4 D^2_{\rm Mpc} S_{\rm CO}\ M_\odot$ (Table 4).

### 3.2. 3 mm *Continuum Emission from UGC 6614*

We searched for 3 mm continuum emission from all the galaxies in our sample. Of the seven galaxies that we observed, two have been detected in radio continuum at 1.4 GHz in the NRAO VLA Sky Survey (NVSS) (Condon et al. 1998); they are UGC 6614 and F568-6. Both galaxies are also strong emitters in the VLA Faint Images of the Radio Sky at Twenty cm (FIRST) Survey (Becker et al. 1995), which is at a similar frequency but has a much higher resolution than NVSS ($\sim$5″).

We detected only UGC 6614 in 3 mm continuum emission using BIMA (Fig. 6); the remaining six galaxies were not detected. Table 5 lists the continuum 3 mm flux observed in UGC

TABLE 4
CO Fluxes and Molecular Gas Masses

| Galaxy Name | BIMA Peak Flux (Jy beam$^{-1}$) | Noise | Channel Width (km s$^{-1}$) | H I Width $W_{50}$ (km s$^{-1}$) | IRAM Flux (Jy km s$^{-1}$) | Noise | Molecular Gas Mass[a] ($M_\odot$) |
|---|---|---|---|---|---|---|---|
| UGC 6614 | 0.060 | 0.017 | 6.1 | 242 | 2.30 | 0.006 | $2.8 \times 10^8$ |
| F568-6 A | 0.043 | 0.013 | 6.1 | ... | 1.86 | 0.005 | $0.7 \times 10^9$ |
| F568-6 B | 0.057 | 0.013 | 6.1 | ... | 5.24 | 0.005 | $1.9 \times 10^9$ |
| UGC 4115 | ... | 0.047 | 6.1 | 83 | ... | ... | $<1.1 \times 10^7$ |
| UGC 5209 | ... | 0.007 | 6.1 | 49 | ... | ... | $<2.4 \times 10^6$ |
| UGC 5585 | ... | 0.039 | 6.1 | 146 | ... | ... | $<1.3 \times 10^7$ |
| UGC 5709 | ... | 0.022 | 6.1 | 247 | ... | ... | $<4.6 \times 10^9$ |
| F583-1 | ... | 0.056 | 6.1 | 174 | ... | ... | $<1.1 \times 10^9$ |

Notes.—The upper limits for the nondetections in BIMA were derived using the noise levels in the corresponding channel maps and the width of the H I line ($W_{50}$). For F583-1, twice the H I rotation curve peak was used (de Blok et al. 2001) for the width of the H I line instead of $W_{50}$.
[a] Molecular gas masses were derived from IRAM fluxes; the values represent gas masses for the detected regions only and not for the entire galaxy.

6614 and upper limits for the remaining galaxies. In UGC 6614 the continuum emission is detected at a mean frequency of 111.2 GHz, and the peak flux at this frequency is 4.9 mJy beam$^{-1}$. The noise in the map is 1.2 mJy beam$^{-1}$, which means that the detection has a signal-to-noise ratio (S/N) of approximately 4. The beam is $\sim 16''$. The position of the peak in the continuum source is R.A. $= 11^h39^m14^s.8$, decl. $= 17^\circ08'37''.5$; the error is $\pm 4''$. Within error limits, the continuum emission peak is definitely coincident with the Two Micron All Sky Survey (2MASS) location of the galaxy center (Table 1). Although the S/N of the detection is not high, the fact that the continuum source is located at the galaxy nucleus raises the significance of the detection.

We calculated the spectral index of the continuum emission for UGC 6614 and upper limits for F568-6 using data from the FIRST 1.4 GHz VLA survey. We convolved the FIRST 1.4 GHz maps of UGC 6614 and F568-6 to the same resolution as the BIMA maps and measured the peak flux. Table 5 lists the spectral index for UGC 6614 and upper limits for F568-6. The spectrum is flat for UGC 6614 ($\alpha \sim 0$, where $f_\nu \propto \nu^\alpha$) and is likely declining at millimeter wavelengths for F568-6. As both galaxies host AGNs and have little star formation activity, the radio continuum emission is probably nonthermal in nature. However, for UGC 6614, we confirmed this by using the H$\alpha$ flux in the galaxy (de Blok & van der Hulst 1998) to derive the star formation rate (SFR) and infrared luminosity (Kennicutt 1983, 1998). The expected 1.4 GHz radio continuum flux from the H$\alpha$ emission is only 0.15 mJy. This is much less than the actual continuum flux measured in the 1.4 GHz map of UGC 6614, which is 5.67 mJy. Thus, the BIMA 3 mm continuum emission from UGC 6614 is nonthermal in nature and due to an AGN in the galaxy. As mentioned earlier, AGN activity in UGC 6614 has been detected at optical wavelengths (Schombert 1998) and also in X-ray emission (*XMM-Newton* archive).

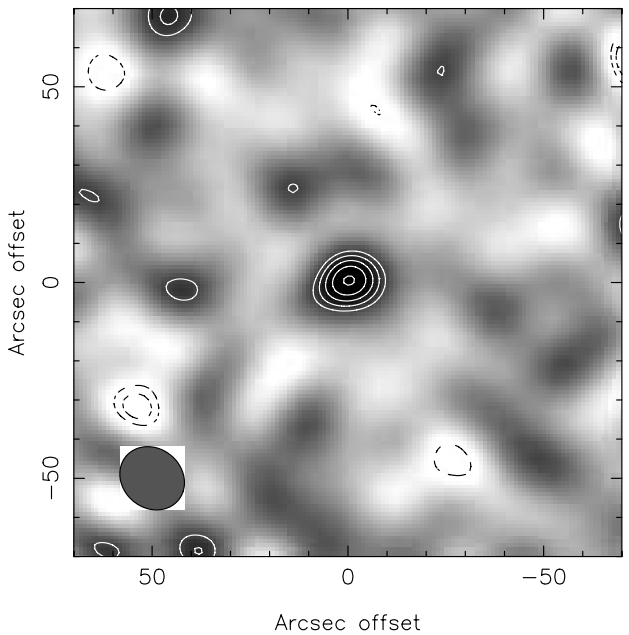


Fig. 6.—BIMA continuum emission map of UGC 6614 at 2.7 mm. The emission is averaged over the upper and lower sidebands, with a mean frequency of 111.2 GHz. The emission is centered on the 2MASS near-infrared position of the nucleus. The beam is shown on the lower left. The emission is contoured at −2, −2.5, 2, 2.5, 3, 3.5, and 4 times the noise level. The noise level is 1.2 mJy beam$^{-1}$, where the beam is $17''.4 \times 15''$. The peak emission is 4.9 mJy beam$^{-1}$.

## 4. DISCUSSION

We have detected CO (1–0) line emission from the disks of two giant LSB galaxies: F568-6 and UGC 6614. We have also detected and mapped the millimeter continuum source in the nucleus of UGC 6614. In the following paragraphs we discuss the implications of our findings.

### 4.1. *Molecular Gas Detection*

As mentioned in § 1, very few LSB galaxies have been detected in CO emission. Of the handful of galaxies in which molecular gas has been detected some are giant, bulge-dominated spiral galaxies with large disk rotation velocities (O'Neil et al. 2000, 2003), while others are more low-mass, disk-dominated systems (Matthews & Gao 2001; Matthews et al. 2005). However, in nearly all previous detections the molecular gas has been found to be centrally concentrated and associated with the galaxy bulge or nucleus, the exception being the single-dish observations of Matthews & Gao (2001), which show CO emission originating from off-center positions for two galaxies in their sample. Our detections of CO emission from UGC 6614 and F568-6 are, however, unique because both detections have interferometric as well as single-dish observations of the molecular gas distribution that clearly indicate that they are associated with the disk and not just the galaxy center. This is important, as it shows that molecular gas can form and exist in the disks of LSB galaxies as well as in their nuclear regions.

TABLE 5
Continuum Fluxes and Spectral Indices

| Galaxy Name | BIMA Continuum Flux[a] (mJy beam$^{-1}$) | Frequency (GHz) | FIRST Continuum Flux[b] (mJy beam$^{-1}$) | Frequency (GHz) | Spectral Index |
|---|---|---|---|---|---|
| UGC 6614 | 4.9 | 111.25 | 5.5 | 1.4 | −0.03 |
| F568-6 | <2.4 | 108.4 | 5.4 | 1.4 | <−0.19 |
| UGC 4115 | <8.4 | 113.5 | ... | ... | ... |
| UGC 5209 | <1.2 | 113.5 | ... | ... | ... |
| NGC 5585 | <6.3 | 113.5 | ... | ... | ... |
| UGC 5709 | <4.5 | 111.3 | ... | ... | ... |
| F583-1 | <10.5 | 112.8 | ... | ... | ... |

[a] The upper limits for the nondetections of BIMA continuum fluxes are given as 3 times the noise levels in the corresponding maps.
[b] The FIRST map is smoothed to the same resolution of the BIMA map before estimating the continuum flux.

Previous studies of LSB galaxies suggest that the low detection rate of molecular gas is a result of a combination of low metallicity and low gas surface density in the disk (van der Hulst et al. 1993; de Blok et al. 1996; Mihos et al. 1999). In addition, LSB galaxies have massive dark halos that may prevent global disk instabilities from forming even when they interact with other galaxies (Mihos et al. 1997); this reduces the formation of shocks that form dense clouds and lead to massive star formation in galaxy disks (Gerritsen & de Blok 1999). In LSB disks the molecular gas may not form due to such large-scale instabilities. Instead it may form due to local instabilities, which will result in isolated clumps of molecular gas and localized regions of modest star formation. Signatures of such localized star formation have been observed in LSB galaxies (Schombert et al. 1990; McGaugh et al. 1995), and our observations of molecular gas in the disks of both UGC 6614 and F568-6 further support this idea. Thus, LSB galaxies may not be as devoid of molecular gas as thought earlier; the distribution may just be localized to isolated regions over the disk and hence difficult to detect.

Another possibility that is hard to exclude is that, given the physical conditions of the interstellar medium in LSB galaxies, the CO to $H_2$ conversion factor is different from the standard value (Mihos et al. 1999; Gerritsen & de Blok 1999). This might allow for substantially more molecular gas to be present than we infer. Bearing this caveat in mind, our observations nevertheless seem to suggest a picture in which molecular gas is rare in LSB galaxies but not completely absent. Such a distribution of molecular gas supports the observed, low-intensity star formation in isolated regions that is seen in these galaxies.

### 4.2. *Continuum Emission*

Figure 6 shows the BIMA map of the continuum source in UGC 6614. The central peak coincides with the 2MASS center of the galaxy; the offset between the two is less than an arcsecond. The emission is probably nonthermal in nature and due to an AGN in the galaxy. Several giant LSB galaxies that have prominent bulges have been found to host AGNs and show weak Seyfert activity. AGN activity in LSB galaxies has been detected in optical emission lines (Schombert 1998; Sprayberry et al. 1995). The nuclear activity is due to the accretion of mass onto a supermassive black hole in the galactic center. It is now widely accepted that most galaxies with a well-defined bulge contain a black hole (Magorrian et al. 1998) and that the bulge mass correlates well with the black hole mass (Ferrarese et al. 2001). Giant LSB galaxies have both prominent bulges and copious amounts of neutral hydrogen (H I) gas in their inner disks. Hence, it is not surprising that these galaxies show signs of AGN activity. However, it is not clear how the gas is transported to the nucleus, since gas fueling processes such as bars are not frequently found in these galaxies (Mihos et al. 1997). It could be that, since the AGN activity is fairly weak in LSB galaxies, the gas torquing produced by the disk spiral arms is enough to funnel gas into the nuclear regions and fuel the AGN.

Very little is known about the continuum emission from LSB galaxies. A handful appear bright in the NVSS and FIRST surveys that are at 1.4 GHz, but none have been studied at millimeter wavelengths (e.g., 100 GHz). The continuum source at 111 GHz in UGC 6614 is the first such detection at millimeter wavelengths. Surprisingly F568-6 is not bright at millimeter wavelengths, although its core is bright in the 1.4 GHz continuum maps (NVSS and FIRST). This implies that the synchrotron spectrum of F568-6 turns over from a flat spectrum to a steeply falling spectrum before millimeter wavelengths, whereas in UGC 6614 it remains constant. A similar difference in turnover frequencies is observed in the nearby Seyfert galaxies NGC 1068 and NGC 3147 (Krips et al. 2006) and is probably due to the different magnetic field strengths in their AGNs (e.g., Krolik 1999). Flat-spectrum radio galaxies also show a variation in turnover frequencies between centimeter and millimeter wavelengths (Bloom et al. 1999), but not many sources are found to be bright at millimeter wavelengths. Thus, UGC 6614 is unique with respect to its nuclear continuum source, which is radio-bright even at millimeter wavelengths.

## 5. CONCLUSIONS

We have searched for molecular gas in a sample of seven LSB galaxies using the BIMA interferometer. Molecular gas was detected in the disks of two galaxies, UGC 6614 and F568-6, using the IRAM 30 m single-dish telescope. Both galaxies have prominent bulges and large, low surface brightness (LSB) disks. Our results indicate that molecular gas may be present in both the disks of LSB galaxies as well as their nuclei, but the distribution is localized over isolated regions and thus difficult to detect in unbiased single-dish observations. Overall, it appears that molecular gas is rare in these galaxies but not completely absent. We have also detected millimeter continuum emission from the nucleus of one of these galaxies: UGC 6614. Our main results are summarized below.

1. CO (1–0) emission was detected in UGC 6614 at approximately 17 kpc (38″) west of the nucleus. It is associated with a spiral feature in the disk. The mass of molecular gas detected from this location is $\sim 2.8 \times 10^8\ M_\odot$. The BIMA observations did not detect any molecular gas in the nuclear region, probably because the gas surface density averaged over the BIMA beam falls below the detection limits of the observation.

2. CO (1–0) emission in F568-6 was detected at two positions in the inner disk. One position is close to the nucleus, and the other is approximately 28 kpc (30″) east of the nucleus. The BIMA intensity maps indicate that the CO (1–0) emission is distributed about the nucleus and extends into the inner disk. The mass of molecular gas associated with the detection is $\sim 2.6 \times 10^9\ M_\odot$.

3. We have also detected a millimeter continuum source in UGC 6614 at the center of the galaxy. Comparing it with VLA FIRST 1.5 GHz maps, we find that it has a flat spectrum between 1 and 110 GHz. The continuum emission is due to the AGN in the galaxy, which has been detected at optical and X-ray wavelengths as well. Millimeter continuum emission from Seyfert or radio-loud galaxies is rare, and so UGC 6614 is fairly unique in its AGN activity compared to most spiral galaxies.

The authors would like to thank Alice Quillen for providing the *R*-band images of UGC 6614 and F568-6. Observations with the BIMA millimeter-wave array are partially supported by NSF grant AST 02-28974. We are grateful to the members of the IRAM staff for their help in the observations. This research has made use of the NASA/IPAC Infrared Science Archive, which is operated by the Jet Propulsion Laboratory, California Institute of Technology, under contract with the National Aeronautics and Space Administration. We also acknowledge the use of the HyperLeda database (http://leda.univ-lyon1.fr).

REFERENCES

Becker, R. H., White, R. L., & Helfand, D. J. 1995, ApJ, 450, 559
Bloom, S. D., et al. 1999, ApJS, 122, 1
Buisson, G., et al. 2002, CLASS Continuum and Line Analysis System Handbook (Grenoble: IRAM), http://iram.fr/IRAMFR/GILDAS/doc/html/class-html/class.html
Condon, J. J., Cotton, W. D., Greisen, E. W., Yin, Q. F., Perley, R. A., Taylor, G. B., & Broderick, J. 1998, AJ, 115, 1693
de Blok, W. J. G., McGaugh, S. S., & Rubin, V. C. 2001, AJ, 122, 2396
de Blok, W. J. G., McGaugh, S. S., & van der Hulst, J. M. 1996, MNRAS, 283, 18
de Blok, W. J. G., & van der Hulst, J. M. 1998, A&A, 336, 49
Ferrarese, L., et al. 2001, ApJ, 555, L79
Gerritsen, J. P. E., & de Blok, W. J. G. 1999, A&A, 342, 655
Impey, C., & Bothun, G. 1997, ARA&A, 35, 267
Kennicutt, R. C. 1983, ApJ, 272, 54
———. 1998, ARA&A, 36, 189
Krips, M., et al. 2006, A&A, 446, 113
Krolik, J. H. 1999, Active Galactic Nuclei: From the Central Black Hole to the Galactic Environment (Princeton: Princeton Univ. Press)
Magorrian, J., et al. 1998, AJ, 115, 2285
Matthews, L. D., & Gallagher, J. S. 1997, AJ, 114, 1899
Matthews, L. D., & Gao, Y. 2001, ApJ, 549, L191
Matthews, L. D., Gao, Y., Uson, J. M., & Combes, F. 2005, AJ, 129, 1849
McGaugh, S. S. 1994, ApJ, 426, 135
McGaugh, S. S., & Bothun, G. D. 1994, AJ, 107, 530
McGaugh, S. S., Schombert, J. M., & Bothun, G. D. 1995, AJ, 109, 2019
Mihos, J. C., McGaugh, S. S., & de Blok, W. J. G. 1997, ApJ, 477, L79
Mihos, J. C., Spaans, M., & McGaugh, S. S. 1999, ApJ, 515, 89
O'Neil, K., Hofner, P., & Schinnerer, E. 2000, ApJ, 545, L99
O'Neil, K., & Schinnerer, E. 2004, ApJ, 615, L109
O'Neil, K., Schinnerer, E., & Hofner, P. 2003, ApJ, 588, 230
Paturel, G., Theureau, G., Bottinelli, L., Gouguenheim, L., Coudreau-Durand, N., Hallet, N., & Petit, C. 2003, A&A, 412, 45
Pickering, T. E., Impey, C. D., van Gorkom, J. H., & Bothun, G. D. 1997, AJ, 114, 1858
Quillen, A. C., & Pickering, T. E. 1997, AJ, 113, 2075
Sault, R. J., Teuben, P. J., & Wright, M. C. H. 1995, in ASP Conf. Ser. 77, Astronomical Data Analysis Software and Systems IV, ed. R. A. Shaw, H. E. Payne, & J. J. E. Hayes (San Francisco: ASP), 433
Schombert, J. M. 1998, AJ, 116, 1650
Schombert, J. M., Bothun, G. D., Impey, C. D., & Mundy, L. G. 1990, AJ, 100, 1523
Scoville, N. Z., & Sanders, D. B. 1987, in Interstellar Processes, ed. D. Hollenbach & H. Thronson (Dordrecht: Reidel), 21
Sprayberry, D., Impey, C. D., Bothun, G. D., & Irwin, M. J. 1995, AJ, 109, 558
Strong, A. W., et al. 1988, A&A, 207, 1
van der Hulst, J. M., Skillman, E. D., Smith, T. R., Bothun, G. D., McGaugh, S. S., & de Blok, W. J. G. 1993, AJ, 106, 548
Welch, W. J., et al. 1996, PASP, 108, 93